Desalination and Water Treatment
www.deswater.com

doi: 10.5004/dwt.2020.26042

196 (2020) 228–237
August

Study of 2,4-D herbicide removal from aqueous solutions using synthesized TiO_2-zeolite nanocomposite by laser irradiation

Fatemeh Abdollah[a], Seyed Mehdi Borghei[b], Elham Moniri[c,*], Salimeh Kimiagar[d], Homayon Ahmad Panahi[e]

[a]*Department of Environmental Engineering, Faculty of Natural Resources and Environment, Science and Research Branch, Islamic Azad University, Postal Code: 14515-775, Tehran, Iran, Tel. +982144865179-82; email: fateme.abdollah@yahoo.com (F. Abdollah)*
[b]*Department of Chemical and Petroleum Engineering, Sharif University of Technology, Postal Code: 11155-1639, Tehran, Iran, Tel. +982166161; email: mborghei@sharif.edu (S.M. Borghei)*
[c]*Department of Chemistry, Varamin (Pishva) Branch, Islamic Azad University, Postal Code: 33817-74895, Pishva, Iran, Tel. +982136725011-14; Fax: +982136724767; email: moniri30003000@yahoo.com (E. Moniri)*
[d]*Nano Research Lab (NRL), Physics Department, Central Tehran Branch, Islamic Azad University, Postal Code: 86831-14676, Tehran, Iran, Tel. +982188074907; email: s.kimia8579@gmail.com (S. Kimiagar)*
[e]*Department of Chemistry, Central Tehran Branch, Islamic Azad University, Postal Code: 86831-14676, Tehran, Iran, Tel. +982188074907; email: panahi20002000@yahoo.com (H.A. Panahi)*

Received 17 August 2019; Accepted 25 April 2020

ABSTRACT

TiO_2/Zeolite composite was synthesized through a sol–gel approach continuously. TiO_2/Zeolite composite was exposed to laser irradiation until conversion to TiO_2/Zeolite nanocomposite (T/Z) and T/Z was modified with m-phenylenediamine (N-T/Z). The resulting N-T/Z was characterized by Fourier transform infrared spectroscopy, scanning electron microscopy, energy dispersive X-ray, dynamic light scattering, and thermogravimetric analysis. The average range of particle size of the N-T/Z was about ~140 nm. The N-T/Z product was evaluated as a sorbent for removing 2,4-D from aqueous solutions. The adsorption operational parameters were investigated in a batch system. The complete removal of 2,4-D was investigated under optimum conditions in real samples by high-performance liquid chromatography. A 2,4-D removal efficiency of 72%–99% was obtained from the river, well, and agricultural drainage water samples. The pseudo-second-order kinetic model fitted the 2,4-D removal, and equilibrium data well followed the Langmuir model. The maximum adsorption capacity of the obtained sorbent was q_{max} = 4.914 mg g^{-1}. The product had excellent stability for reprocessing in several runs without losing adsorptivity significantly.

Keywords: Water pollution; Nanocomposite; 2,4-D; Isotherm; Kinetic; Real sample; Reusable sorbent

1. Introduction

The presence of pesticides in freshwater resources is a serious threat to human health and the environment. The use of these compounds has been widely extended in agricultural activities. The 2,4-Dichlorophenoxyacetic acid (2,4-D), categorized as a phenoxy/anionic herbicide, is commonly used to control broadleaf weeds in agriculture, garden, forestry, and aquatic vegetation [1–3] owing to its low cost and excellent selectivity. The consumption

* Corresponding author.

rate of herbicides in Iran is reported about 530 tons per year, with 20%–30% claimed by the 2,4-D compound [4]. Due to its water solubility, high mobility, a high rate for leaching, and low soil adsorption coefficient, 2,4-D residues have been reported in aquatic ecosystems [5–7]. This compound is considered as a toxic chemical with harmful impacts on human health [8,9]. It is also known as an endocrine disruptor and can lead to carcinogenic effects on mammals [10]. The maximum permissible concentration of 2,4-D is recommended 30 ppb in drinking water [11]. Due to poor biodegradability [12], and since conventional water treatment processes cannot efficiently remove 2,4-D, there is a significant need to remove this pollutant from water bodies. Thus, several methods have been developed for the 2,4-D removal such as photodegradation [13], biological oxidation [14], advanced oxidation processes (AOPs) [15], nanotubes, and nanocomposites hydrogel as sorbent materials [16,17] as well as adsorption process on sorbent surfaces [18–20]. Photodegradation of herbicide paraquat under visible and solar light using magnetically recoverable biochar supported ternary heterojunction proved to be effective in degradation and mineralization of the herbicide as well as the photo-reduction of carbon dioxide into methane [21–23].

Among all of the suggested methods, the conventional adsorption technique has reduced mobility and reaction time without any harmful by-products, which has mostly been investigated for adsorption of dyes in aqueous media [24]. Thus, it could affect the control of the fate of 2,4-D in both terrestrial and aquatic environments. TiO_2 semiconductor can be used to remove pollutants through adsorption onto surfaces alongside the photocatalytic oxidation process [25,26]. The use of TiO_2 nanoparticles as an adsorbent/photocatalyst is limited by the aggregation of particles in aquatic media. To overcome these problems, various concerted efforts have been suggested to immobilize TiO_2 particles on different supports, particularly natural substrates such as diatomite [27], montmorillonite [28], silica [29], kaolinite [30], and zeolite [31]. Among various materials, zeolite could be one of the most suitable materials for supporting TiO_2, thanks to its unique porous structure, excellent adsorption capacity, and special ion-exchange ability [32,33]. Clinoptilolite is a kind of low-cost, abundant porous aluminosilicate mineral among the natural zeolite group. Hence, degrading different environmental pollutants by TiO_2-zeolite composite has been studied by several researchers [25,34]. Sol–gel, solvothermal, and hydrothermal methods are among the conventional methods for synthesizing TiO_2/zeolite composites.

In this research, TiO_2/zeolite composite was synthesized by the sol–gel method and exposed to laser irradiation until being converted to nanocomposite (T/Z). Then, it was modified with the aminic organic ligand for adsorption of 2,4-D from an aqueous solution. The pH, contact time, temperature on sorption, and reusability were examined. Furthermore, adsorption isotherms as well as the sorbent kinetics were also explored. Finally, 2,4-D extraction from real samples such as well water, river water, and agricultural drainage water was studied via the high-performance liquid chromatography (HPLC) method.

2. Experimental

2.1. Materials

The natural zeolite clinoptilolite was purchased from Semnan, Iran. TiO_2, dimethylformamide (DMF), dried acetone (maximum 0.005% H_2O), methanol, acetonitrile for chromatography, as well as salt and inorganic acid were purchased from Merck (Darmstadt, Germany). 1,1′-carbonyldiimidazole (CDI), m-phenylenediamine were purchased from Sigma-Aldrich (St. Louis, MO, USA). Analytical grade solvents such as methanol, acetone, and DMF were used as received. A stock of 2,4-D solution was daily prepared by dissolving 0.01 g of 2,4-D in 100 mL deionized water on a magnetic stirrer for 3 h.

2.2. Instruments

The FT-IR spectra were captured using a KBr disk method at room temperature with FT-IR-410 (JASCO, Japan) within the range of 4,000–400 cm^{-1}. The particle size distribution histograms of N-T/Z nanocomposite were captured by dynamic light scattering (DLS, Malvern Instruments Ltd., UK, MAL 1008078). The morphology, size, and percentage of elements of N-T/Z nanocomposite were obtained through scanning electron microscopy (SEM) and energy-dispersive X-ray spectroscopy (EDX, VEGA/TESCAN-XMU, Brno – Czech Republic). Thermogravimetric analysis (TGA) was conducted using a TGA-50H (Shimadzu Corporation, Kyoto, Japan) within the range of 0°–600°C at a heating rate of 10°C min^{-1} under an air atmosphere. The 2,4-D concentration was assayed within the range of 200–400 nm by a UV-Vis spectrophotometer (Perkin Elmer/Lambada 25 UV/Vis Spectrophotometer, USA). The HPLC system was used for determining the 2,4-D concentration in the real samples.

2.3. T/Z nanocomposite synthesis

The T/Z nanocomposite was synthesized via the sol–gel method with a 1:1 weight ratio of TiO_2 anatase. Specifically, zeolite clinoptilolite in 15 mL of deionized water was stirred at 40°C for 4 h until a milky white solution was reached. Then, the solution was exposed to irradiation of an ND:YAG pulsed laser system (Quantel, Brilliant b class 4 with 532 nm wavelength with 5 ns pulse duration, 10 Hz repetition rate, 90 mJ maximum pulse energy, and 7 mm beam diameter). The optimum size of the nanocomposite product was obtained after 7 min of laser irradiation [35]. Finally, the product was dried at room temperature.

2.4. Modification of T/Z nanocomposite by 1,1′-carbonyldiimidazole

In this step, 3.0 g T/Z nanocomposite was dried inside an oven at 100°C for 1 h. The resulting T/Z nanocomposite was washed twice with dried acetone and dried at room temperature. The obtained T/Z nanocomposite powder (3.0 g) was added to dried acetone (20 mL) and 1,1′-carbonyldiimidazole (CDI) (0.1 g) which was stirred for 3 h at room temperature. Subsequently, the above solution of

the mixture was discharged, and the remained product was used for the next step.

2.5. Modification of T/Z nanocomposite by m-phenylenediamine

The precipitate from the last step (3.0 g T/Z nanocomposite, and about 0.1 g of 1,1′-CDI) was dissolved in DMF (50 mL), dried acetone (20 mL) and m-phenylenediamine (0.3 g). The solution was kept at 4°C under stirring. After 30 h, the solution obtained was stirred at room temperature for 8 h. The final product was separated and the sediment obtained was washed two times with DMF (20 mL). The modification processes are summarized in Fig. 1.

2.6. Batch adsorption study

A series of micro-tubes containing 0.01 g of N-T/Z nanocomposite samples were used for the batch experiment in a vortex in the presence of 1.5 mL of 2,4-D solution and fixed pH = 6. After sufficient time for the adsorption process (30 min), the sorbent was separated through centrifugation at 6,000 rpm within 10 min. The UV-Vis spectroscopy determined the concentration of 2,4-D within the supernatant. The spectra were recorded within the range of 200–400 nm, with the 2,4-D maximum absorption at λ_{max} = 283 nm.

The level of 2,4-D herbicide uptake by the N-T/Z nanocomposite was calculated from the difference between the initial (C_0, mg L^{-1}) and equilibrium (C_e, mg L^{-1}) concentrations of 2,4-D using the following equation:

$$\text{Removal } \% = \left[\frac{\left(C_0 - C_e\right)}{C_0}\right] \times 100 \tag{1}$$

The removal efficiency (Eq. 1) and the content adsorbed by N-T/Z product (Eq. 2) were considered as follows:

$$Q = \left(C_0 - C_e\right)\frac{V}{M} \tag{2}$$

where Q (mg g^{-1}), V (L), and M (g) are adsorbed 2,4-D, volume of 2,4-D solution and the mass of N-T/Z, respectively. The average value of the triplicate experiment reported in this study.

2.7. Reusability

The reusability of the synthesized N-T/Z was studied under the optimum condition obtained from the above experiments. For each run, 10 mg L^{-1} of 2,4-D (1.5 mL) at pH = 6.0 and 0.01 g of N-T/Z were vortexed for 15 min and collected through centrifugation for 5 min. The concentration of 2,4-D was determined by a UV-Vis spectrophotometer (R_1 run).

Next, 1.5 mL pure methanol was added to N-T/Z and was shaken for 10 min at 50°C. The samples were subsequently centrifuged for 5 min for further use. The experiment proceeded with the same previous conditions to reach the R_9 run.

2.8. Isotherm studies

To obtain the isotherm adsorption, firstly, 100 mg L^{-1} of the 2,4-D solution was prepared at ambient temperature (stock solution). Then, diluted 2,4-D solution (5–80 ppm) was added to the samples of micro-tubes with an invariant (constant) amount of N-T/Z nanocomposite (10 mg) for isotherm

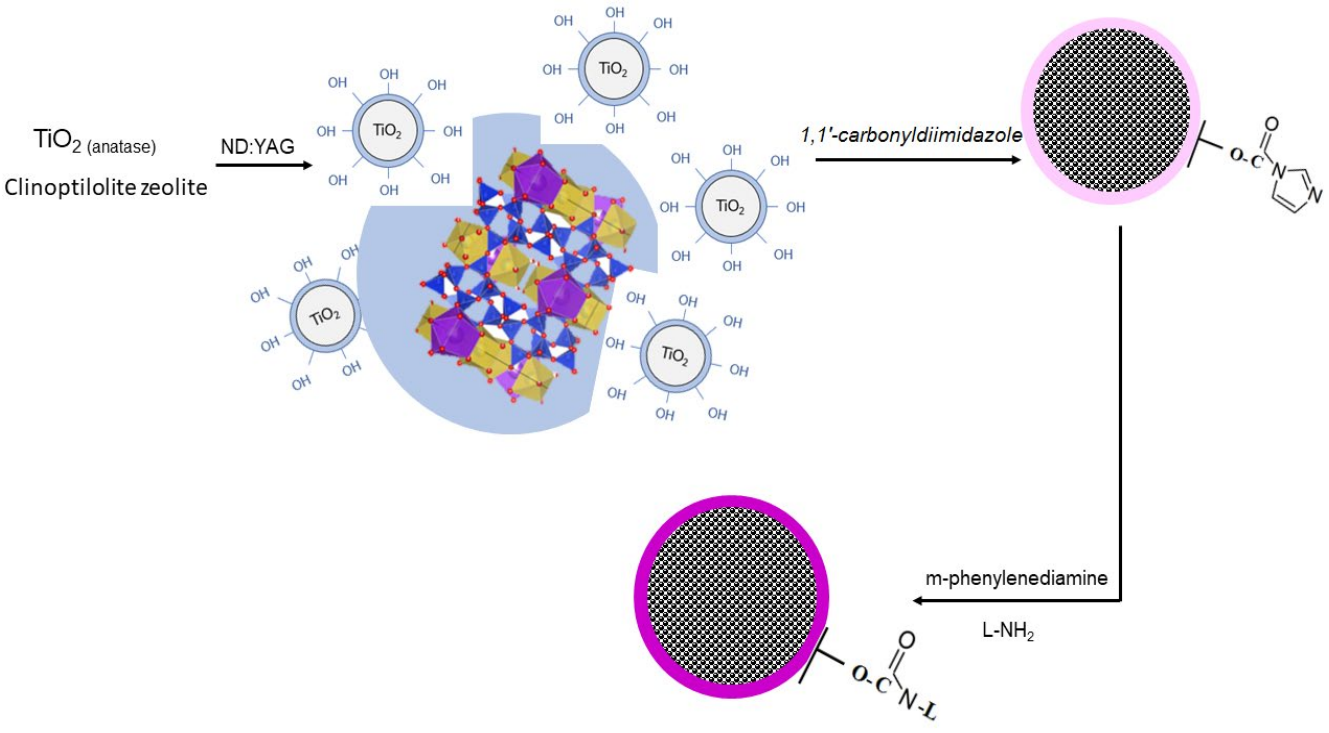

Fig. 1. Schematic presentation of modified N-T/Z.

studies at a fixed temperature (20°C ± 5°C at pH = 6). The micro-tubes were vortexed (200 rpm–30 min) and the samples were centrifuged (6,000 rpm–10 min). The 2,4-D concentration was determined by a UV-Vis spectrophotometer. The equilibrium concentration of 2,4-D was calculated by Eq. (2).

2.9. Kinetic studies

For the kinetic experiments, at conditions of 20 mg L^{-1} with 1.5 mL of 2,4-D, pH = 6.0, and 0.01 g N-T/Z, the samples were vortexed for different time intervals (2–60 min). They were then centrifuged for 10 min at 6,000 rpm, and the concentration of 2,4-D was determined by a UV-Vis spectrophotometer.

2.10. HPLC assay

The 2,4-D concentration in real samples (well water, river water, and agricultural drainage water) was determined via HPLC (KNAUER, Germany) using 2500 ultraviolet (UV) detector at 283 nm wavelength of 2,4-D. The isocratic mobile phase was a mixture of acetonitrile and water with a rate of flow of 0.5 mL min^{-1}. The stationary phase was a C_8 column (250 mm × 4.6 mm, with 5 μm particle size). The retention time for the 2,4-D peak was 3.5 min. Five levels of 2,4-D (1–7 ppm) were considered for the calibration curve.

2.11. Batch assay of 2,4-D for real samples

Firstly, the real samples were filtered via a Whatman filter paper (No. 42). Several solutions (1.5 mL) containing 5 mg L^{-1} of 2,4-D were prepared in a micro-tube after regulating the pH to the optimum value (6). N-T/Z nanocomposite (0.05 g) was added to the micro-tube and vortexed for 30 min. The samples were then centrifuged for 10 min with 6,000 rpm. The concentration of 2,4-D was evaluated using the HPLC technique.

3. Results and discussion

3.1. Characteristics of N-T/Z

The FT-IR spectrum of the modified T/Z nanocomposite with m-phenylenediamine is shown in Fig. 2b. Double absorption peaks at 516 and 694 cm^{-1} were related to Ti–O stretching vibration. Another sharp peak at around 1,064 cm^{-1} was related to the asymmetric stretching vibrations of Si–O, which was covered with Al–O–Si and Al–O stretching vibrations in the clinoptilolite zeolite. This absorption band indicated that TiO_2 molecules bond at the surface of the zeolite framework [36,37]. The peak at 1,639 cm^{-1} was associated with the C=O groups of 1,1 carbonyl diimidazole. The peaks observed at 1,457; 3,428; and 1,199 were explained by CH_2, NH_2, and C–N functional groups, respectively. These results indicate that the surface treatment through m-phenylenediamine was successful, and *N*-groups entered the interlayer space of the N-T/Z. As shown in Fig. 2a, all the sorbent nanocomposite functional peaks were preserved after the adsorption process of 2,4-D. The additional peaks at ~1,384 and 1,740 cm^{-1} signal the characteristic absorption band corresponding to the phenolic C–O and carboxylic C=O in 2,4-D structure, respectively [38,39]. DLS was employed to determine the particle size of N-T/Z (Fig. 2c). The average particle size was observed about 140 nm, as also confirmed by the results of SEM.

The thermal behavior of the N-T/Z was evaluated via thermal gravimetric analysis (TGA), as shown in Fig. 2d. The decomposition of N-T/Z occurred in three consequent steps. The first weight loss occurred at 150°C (around 3%), which is related to the evaporation of the adsorbed water and dehydration O–H groups on the surface. The second weight loss was observed within the range of 150°C–400°C (around 2%). This can be explained by water evaporation from the inner/inter-dimensional crystal structure on the N-T/Z structure. The third weight loss was found up to 400°C (around 2.5%), which is owing to the degradation of the organic section in the N-T/Z. It is also found that the organic modification was successfully accomplished on N-T/Z nanocomposite. Thus, the results obtained from TGA confirmed that the synthesized N-T/Z was stable until 400°C.

The surface and morphology characterization of N-T/Z was carried out via SEM (Fig. 3).

The surface morphology of the N-T/Z shows porous structures. The SEM images of the N-T/Z after 2,4-D adsorption confirm the maintenance of the porous structure with successful desorption of the analyte on the sorbent surface (Figs. 3c and d). The porous structure helps in adsorbing the 2,4-D herbicide from the surface even following the adsorption process. The reusability study also confirms the application of the N-T/Z sorbent product as reported during nine cycles (see Fig. 7).

The EDS results from the T/Z and N-T/Z are presented in Table 1.

The presence of Al, Si, Ti, C, N, and O elements confirm the successful synthesis of the N-T/Z sample. As shown, there is no signal for carbon and nitrogen elements in the T/Z nanocomposite. Comparing T/Z with N-T/Z, the amount of Si, Al, and Ti diminished with larger carbon and nitrogen contents on the surface of N-T/Z. Meanwhile, the presence of carbon and nitrogen elements after modification of T/Z is another reason for successful synthesis of N-T/Z.

3.2. Optimization of adsorption parameters

The following parameters were optimized for the adsorption process in this study as follows: (a) solution's pH levels, (b) different adsorption times, and (c) temperature changes on the adsorption of 2,4-D on N-T/Z.

The solution's pH level within 3–9 was investigated by the batch method (Fig. 4). The optimum pH amount for 2,4-D adsorption was selected in acidic pH (pH = 6.0). Under acidic conditions, the percentage removal of 2,4-D is higher than that in alkaline conditions [18]. This is owing to the combined effect of point of zero charge (pH_{zpc}) of the final structure of the N-T/Z absorbent and primary structure form of 2,4-D. The zeta potential of N-T/Z is positive. When $pH < pH_{zpc}$, the N-T/Z surface would have a positively charged surface, while at $pH > pH_{zpc}$, the opposite phenomenon will occur.

On the other hand, the pK_a of 2,4-D is 2.7–2.8 [40,41]. Hence, the structure of 2,4-D remains as its initial form in acidic environments and is adsorbed by the N-T/Z adsorbent, where the surface of N-T/Z is positive charged. As the pH

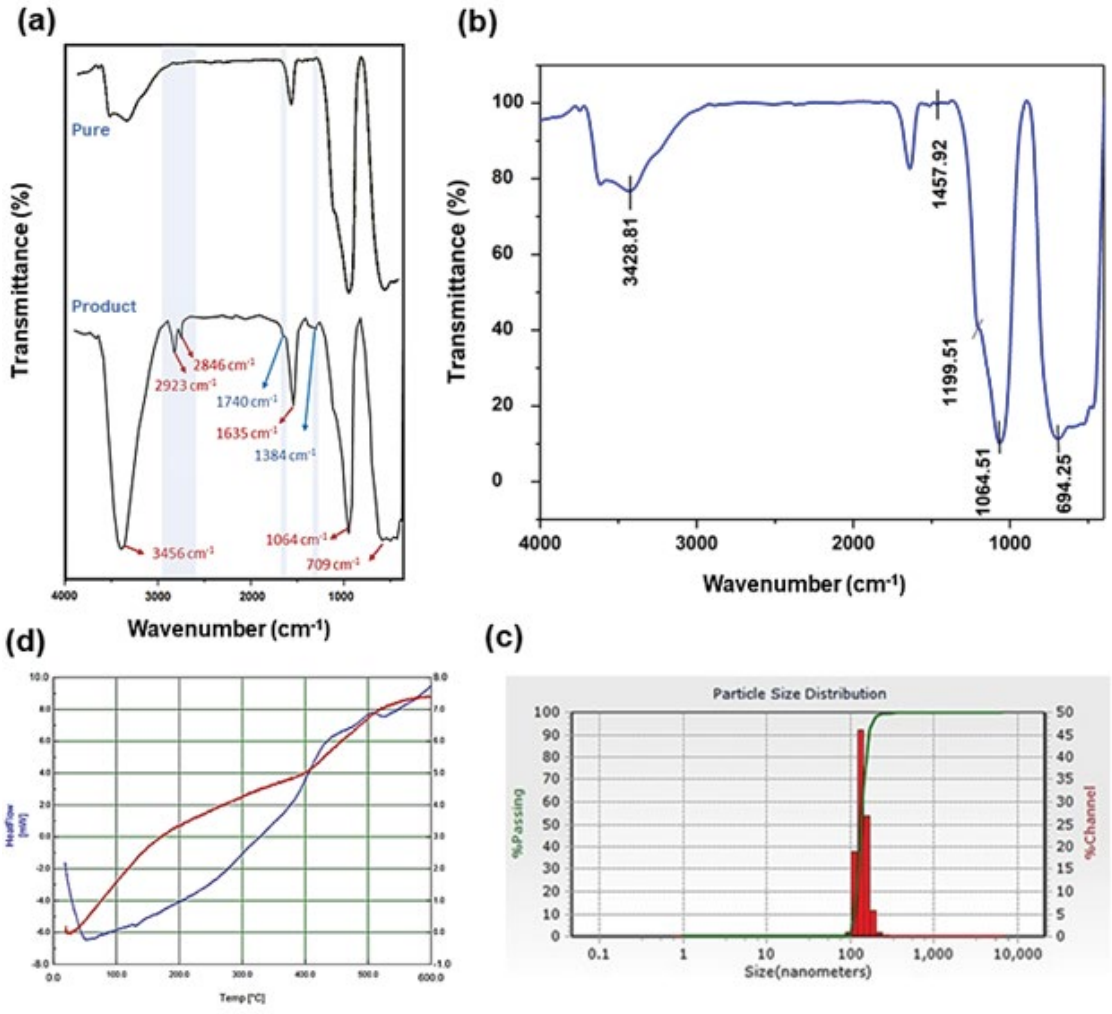

Fig. 2. Characteristics of N-T/Z (a) FTIR spectra of pure and sorbent product after 30 min adsorption of 2,4-D, (b) FTIR of N-T/Z sorbent product, (c) DLS, and (d) TGA analysis of the final product.

Table 1
EDS spectrum data

Samples	T/Z	N-T/Z
Al	5.97	1.63
Si	39.21	28.01
Ti	3.32	2.48
C	N.D	6.00
N	N.D	0.02
O	48.77	61.51
K	1.32	0.19
Ca	1.41	0.16

N.D: Not detected.

value increased, the adsorption of 2,4-D decreased, which can be ascribed to the dominant anionic form of 2,4-D molecules. Thus, the removal percentage of 2,4-D was higher than that at a lower pH. The optimum pH (pH = 6) was selected for the other experiments in this study.

The kinetic study of 2,4-D adsorption at pH 6 with the N-T/Z at a different time is shown in Fig. 5. As observed, the sorption rate of the N-T/Z for 100% saturation sorption was reached after about 10 min. This adsorption rate was approximately 80% in 5 min reaction time. The 2,4-D adsorption rate increased quickly over time. This can be assigned to the accessibility of the binding adsorption active sites on the N-T/Z.

The effect of different temperatures was evaluated under a pH of 6.0 (Fig. 6). As observed, the change in temperature (30°C–50°C) have had no effect on 2,4-D adsorption and, accordingly, the removal efficiency. As the temperature rose beyond $T > 40$°C, the mobility of the analyte increased, so the adsorption process took place at a slightly higher rate compared to the room temperature. This can be considered as a positive aspect of the synthesized adsorbent product, that is, the change of temperature will not alter the removal efficiency of the 2,4-D considerably. The temperature stable adsorption process of 2,4-D onto the N-T/Z sorbent can be used within the temperature range of 30°C–50°C for agricultural drainage water treatment in vast areas.

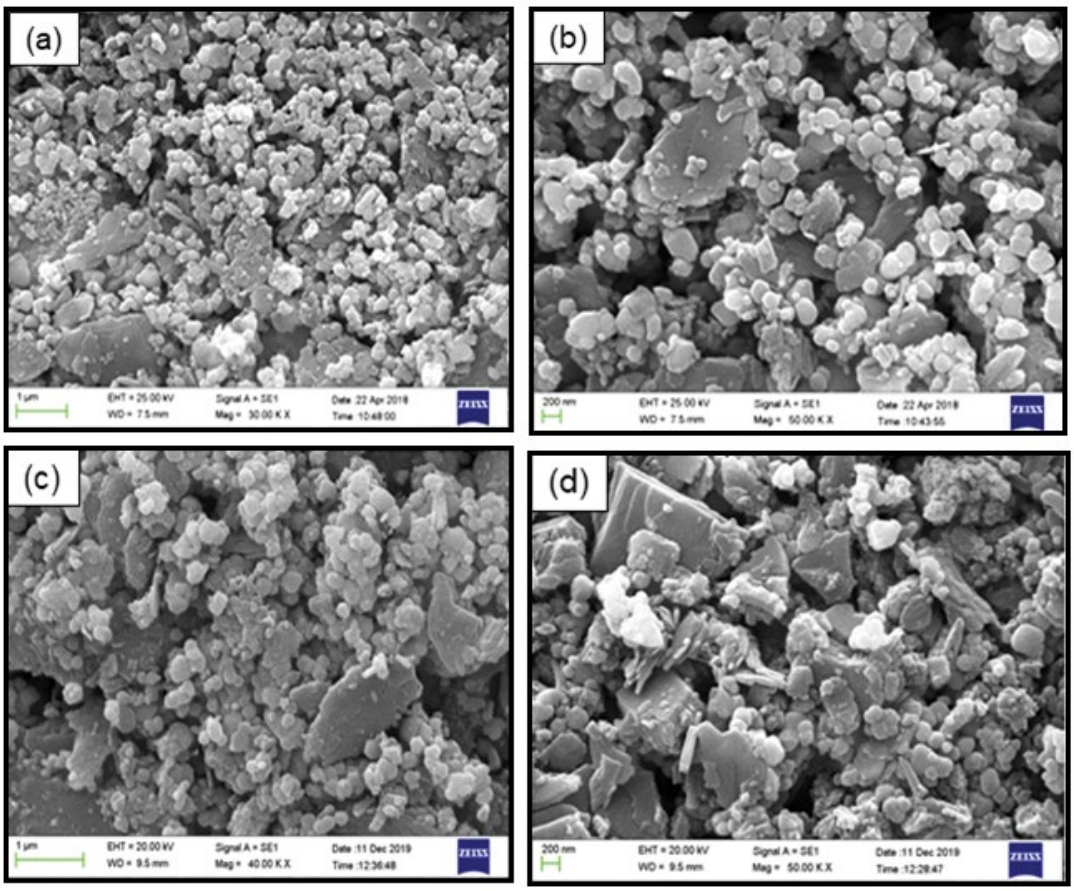

Fig. 3. (a and b) SEM images of N-T/Z sorbent product and (c and d) after 2,4-D adsorption.

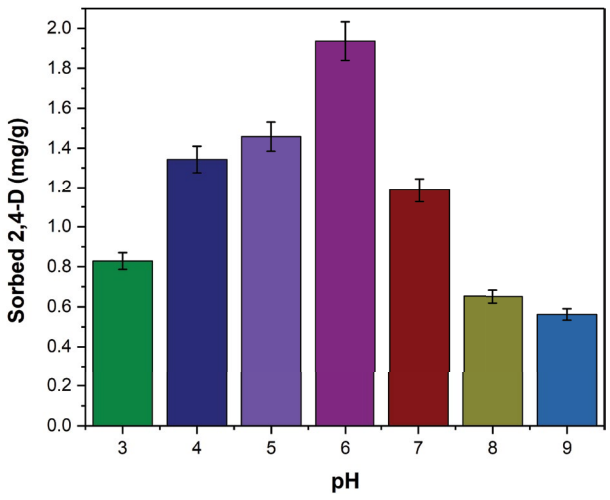

Fig. 4. Effect of pH on sorption of 2,4-D onto N-T/Z.

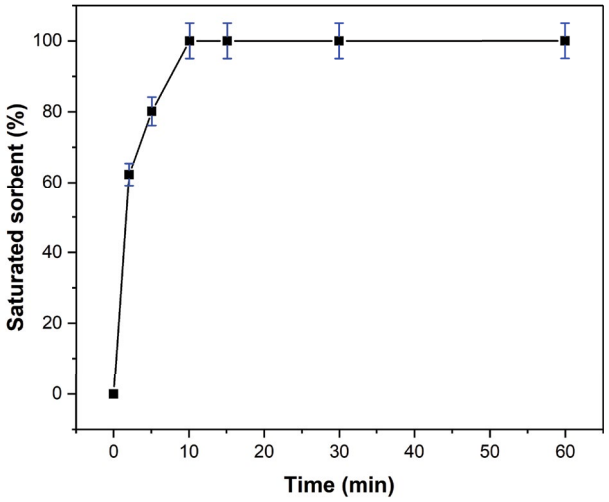

Fig. 5. Kinetic of sorption of 2,4-D onto N-T/Z.

3.3. Reusability

The stability of N-T/Z was assessed for nine consecutive runs under the optimal conditions, and the same experimental circumstances (Fig. 7). There was no reduction in the adsorption efficiency observed for the 2,4-D removal up to the fifth run, and it remained at 100%. The removal efficiency value was found around 90% after nine runs adsorption experiments, showing a slight decrease of 10%. The deterioration of the active sites of N-T/Z can be the main reason for this decline. On the other hand, contamination of the sorbent surface might have occurred through

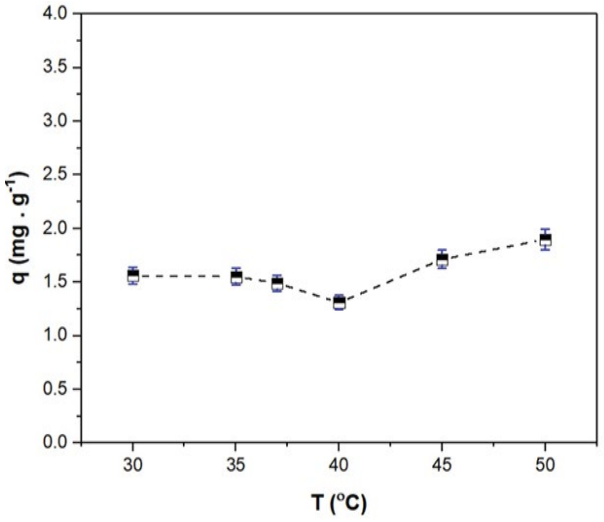

Fig. 6. Effect of temperature on sorption of 2,4-D onto N-T/Z.

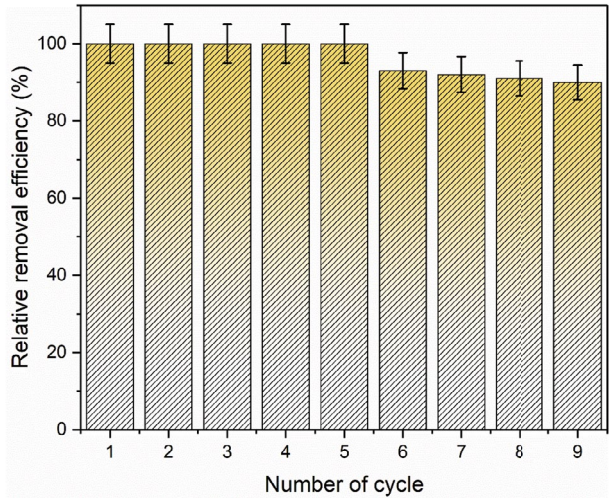

Fig. 7. Reusability of N-T/Z sorbent product.

adsorption of organic compounds, leading to a drop in the adsorbing activity through saturating the active surfaces [1,42]. However, the synthesized N-T/Z exhibited excellent stability for reuse in several runes without any significant drop in the absorbent activity. Note that the reusability of the N-T/Z absorbent is high. Thus, it will definitely compete with other sorbents for removal of 2,4-D in practical applications.

3.4. Adsorption isotherms

Adsorption isotherms revealed a relationship between the 2,4-D as an adsorbate molecule and the N-T/Z solid-phase adsorbent in the solution. In this study, four isotherm models, including Langmuir, Freundlich, Temkin, and Redlich–Peterson, have been analyzed for 2,4-D adsorption on N-T/Z. The best results occur when the coefficient is close to 1 [16]. The Langmuir adsorption isotherm model supposes that only one species is adsorbed to an adsorption site and that adsorption occurs in a monolayer on the adsorbent surface. The Langmuir equation is as follows [43,44].

$$\frac{C_e}{q_e} = \left(\frac{1}{q_{\max}} K_L\right) + \left(\frac{C_e}{q_{\max}}\right) \tag{3}$$

where $q_{\max}$ is the maximum adsorption capacity for 2,4-D, related to the full coverage of a layer on the adsorbent surface of N-T/Z (mg g^{-1}). The $q_{\max}$ here was 4.914 mg g^{-1}. About 4.914 mg of herbicide was adsorbed per gram of the adsorbent. K_L is a constant Langmuir (L mg^{-1}). R_L denotes a dimensionless separator factor. The R_L equation is as follows [45].

$$R_L = \frac{1}{\left(1 + K_L C\right)} \tag{4}$$

where R_L values show how effective the adsorption is: (R_L = 0), irreversible adsorption, (0 < R_L < 1), optimum adsorption, (R_L = 1) linear adsorption and (R_L > 1) undesirable adsorption. Table 2 shows R_L = 0.181 indicating desirable adsorption of 2,4-D herbicide on N-T/Z.

The Freundlich isotherm is experimentally defined for heterogeneous systems. In this model, unlike the Langmuir isotherm, multilayer adsorption occurs on heterogeneous surfaces. The Freundlich equation is as follows [46].

$$\ln_{q_e} = \ln K_F + \frac{1}{n} \ln C_e \tag{5}$$

where K_F is Freundlich constant [(mg g^{-1}) (L $mg^{-1})^{1/n}$], and 1/n denotes the heterogeneity factor. Distribution of adsorption sites towards a homogeneous surface is probable as the 1/n goes towards unity. In Freundlich, the logarithmic reduction of adsorption enthalpy was owing to the enhanced occupancy in a fraction of active sites. The value for 1/n was 0.52. It is concluded that the N-T/Z has a homogeneous surface.

The Temkin adsorption isotherm model explained a linear reduction in the adsorption heat owing to the increase in the number of particles adsorbed on the adsorbent surface. The Temkin equation is as follows [47]:

$$q_e = B \ln A + B \ln C_e \tag{6}$$

where A is Temkin bonding constant (L g^{-1}), indicating the maximum bonding energy. The B parameter is Temkin constant, related to heat adsorption (J mol^{-1}), with the equation being $B = RT/b$, where R is the general gas constant, equal to 8.314 (J mol^{-1} K^{-1}), T represents the absolute temperature (K), and b is heat adsorption.

Redlich–Peterson adsorption isotherm has three constant parameters, A, B, and g (0 < g < 1), and has the following equation [48]:

$$\ln\left[AC_e\left(g_e\right) - 1\right] = \ln C_e + \ln B \tag{7}$$

Adsorption-related parameters of 2,4-D by N-T/Z adsorbent with linear regression are reported in Table 2. According

Table 2
Isotherm parameters for 2,4-D adsorption onto N-T/Z

Isotherm model	Parameter	Quantity
Langmuir	q_{max} (mg g^{-1})	4.914
	K_L (L mg^{-1})	0.056
	R_L (g mg^{-1})	0.181
	R^2	0.995
Freundlich	K_F [(mg g^{-1})(L mg^{-1})$^{1/n}$]	0.52
	n (L mg^{-1})	1.92
	R^2	0.987
Temkin	A (L g^{-1})	0.55
	B	1.078
	b (J mol^{-1})	2,298.182
	R^2	0.991
Redlich–Peterson	A (L g^{-1})	0.298
	B (L mg^{-1})	0.0642
	g	1.005
	R^2	0.993

to the Redlich–Peterson adsorption isotherm, g value was approximately 1, suggesting that the relation between 2,4-D and N-T/Z adsorbent was closer to Longmuir isotherm and followed this equation.

3.5. Adsorption kinetics

The equilibrium data were fitted to the pseudo-first-order and pseudo-second-order kinetic equations. The Lagergren's pseudo-first-order kinetic model [49] can be expressed by Eq. (8):

$$q_t = q_e\left(1 - e^{-k_1 t}\right) \tag{8}$$

where k_1 (min^{-1}) represents the pseudo-first-order kinetic rate constant. Contrary to the pseudo-first-order kinetic model, Ho's pseudo-second-order model [50] is derived in its non-linear form as Eq. (9):

$$q_t = \frac{q_e^2 k_2 t}{1 + q_e k_2 t} \tag{9}$$

where k_2 (g mg^{-1} min^{-1}) is the pseudo-second-order kinetic rate constant. The initial sorption rate, h (mg g^{-1} min^{-1}) regarded as q_t when t approaches zero, is given by Eq. (10):

$$h = k_2 q_e^2 \tag{10}$$

The kinetic parameters obtained from models are listed in Table 3. The adsorption of 2,4-D onto N-T/Z was best described by the pseudo-second-order kinetic model, with the highest R^2 = 0.999. This model could also predict the experimental data reasonably. A high R^2 value indicates the model's success in describing the kinetic data adsorption. The pseudo-second-order model is based on the adsorption loading of the solid phase and predicts the behavior over the entire range of the adsorption process [51].

Table 3
Kinetic parameters for 2,4-D adsorption onto N-T/Z

Kinetic model	Parameter	Quantity
Pseudo-first-order	q_e (mg g^{-1})	0.389
	K_1 (min^{-1})	0.158
	R^2	0.837
Pseudo-second-order	q_e (mg g^{-1})	0.751
	K_2 (g mg^{-1} min^{-1})	1.761
	R^2	0.999

3.6. Method application

The efficiency of the N-T/Z absorbent was evaluated for the removal of 2,4-D in three real samples under the same conditions (Table 4). The three samples included (a) groundwater sample from the well in Lavasanat (North of Tehran, Iran); (b) surface water sample from the Karaj river (Tehran, Iran), and (c) agricultural drainage water (Shahr-e-Ray, South of Tehran, Iran). The results obtained by HPLC are presented in Table 4. The 2,4-D removal efficiency decreased from 100% in deionized water to 99.2%, 76.19%, and 72.15% in agricultural drainage water, well water, and Karaj river, respectively.

This reduction can be related to the complex matrices and interfering functions with competitive tendencies to occupy the active sites on the synthesized sorbent compared to the 2,4-D analyte.

Three real samples contain different organic compounds. The active sites available on the adsorbent surface cannot adsorb all organic compounds; thus, a competitive state develops between 2,4-D and organic compounds for adsorption on the adsorbent. Alternatively, owing to the presence of organic compounds in the spring season, when the sampling experiments of this study were performed, the removal efficiency of the 2,4-D dropped dramatically.

The repetitive procedures of the method suggested in this work with high precision can be confirmed by the low RSD value for 2,4-D adsorption from real samples.

3.7. Comparison of N-T/Z with other reported adsorbents

Table 5 compares the results of 2,4-D removal by different adsorbents obtained here and in previous studies. The developed method provided a superior high removal efficiency (100%) and a far shorter reaction time (10 min) as compared with other developed materials. Further, the pH level of 6 was suitable as it was near the neutral condition, which was similar to the pH of the agricultural drainage water.

4. Conclusion

In this research, m-phenylenediamine as an aminic organic ligand was successfully synthesized on the surface of TiO_2/Zeolite nanocomposite. The N-T/Z product was used as a sorbent to remove 2,4-D from aqueous solutions in real samples (well water, river water, and agricultural drainage water) in a batch system.

Table 4
Determination of 2,4-D in various real samples

HPLC sample	2,4-D (mg L^{-1})	Added (mg L^{-1})	Found (mg L^{-1})	Removal (%)	RSD (%)
Well water	5	0.05	1.21 ± 0.008	76.19	1.89
River water	5	0.05	1.40 ± 0.005	72.15	1.69
Agricultural drainage water	5	0.05	5.00 ± 0.004	99.2	1.06

Table 5
Comparative summary of various adsorbents for removal of 2,4-D

Adsorbent	pH	Reaction time (min)	Removal (%)	Reference
LDH[a]	4.0	50	69	[52]
Granular activated carbon	3.0	60	68	[53]
BFA[b]	3.5	360	87.64	[20]
N-T/Z	6.0	10	72–100	This study

[a]Layered double hydroxide.
[b]Bagasse fly ash.

Several adsorption parameters were investigated and optimized in the removal of the 2,4-D analyte. The results revealed that the overall removal of 2,4-D on the N-T/Z sorbent was optimal at pH = 6.0 (acidic condition) during 10 min of contact following the pseudo-second-order rate model (1.761 min^{-1}, R^2 = 0.999). Various adsorption isotherms were also studied, with the Langmuir model presenting an excellent model fit (R^2 = 0.995) with the maximum adsorption capacity of q_{max} = 4.914 for N-T/Z in adsorbing 2,4-D. The N-T/Z product exhibited high stability after consecutive utilization for nine cycles confirming its high application potential in practical water and wastewater treatment. Accordingly, the N-T/Z nanocomposite sorbent reported in this study demonstrated the advantages of high adsorption capacity, excellent usability, and high chemical stability which could be effective in the advanced wastewater treatment.

References

[1] N. Jaafarzadeh, F. Ghanbari, M. Ahmadi, Catalytic degradation of 2,4-dichlorophenoxyacetic acid (2,4-D) by nano-Fe_2O_3 activated peroxymonosulfate: influential factors and mechanism determination, Chemosphere, 169 (2017) 568–576.

[2] Y. Wang, C. Wu, X. Wang, S. Zhou, The role of humic substances in the anaerobic reductive dechlorination of 2,4-dichlorophenoxyacetic acid by *Comamonas koreensis* strain CY01, J. Hazard. Mater., 164 (2009) 941–947.

[3] Y. Tang, S. Luo, Y. Teng, C. Liu, X. Xu, X. Zhang, L. Chen, Efficient removal of herbicide 2,4-dichlorophenoxyacetic acid from water using Ag/reduced graphene oxide co-decorated TiO_2 nanotube arrays, J. Hazard. Mater., 241–242 (2012) 323–330.

[4] Statistical Centre of Iran, Agricultural Statistic Report 1391, Agricultural Ministry, Tehran, Iran, 2012.

[5] E.R. Bandala, M.A. Peláez, D.D. Dionysiou, S. Gelover, J. Garcia, D. Macías, Degradation of 2,4-dichlorophenoxyacetic acid (2,4-D) using cobalt-peroxymonosulfate in fenton-like process, J. Photochem. Photobiol., A, 186 (2007) 357–363.

[6] A. Boivin, S. Amellal, M. Schiavon, M.T. Van Genuchten, 2,4-Dichlorophenoxyacetic acid (2,4-D) sorption and degradation dynamics in three agricultural soils, Environ. Pollut., 138 (2005) 92–99.

[7] N. Jaafarzadeh, F. Ghanbari, M. Ahmadi, Efficient degradation of 2,4-dichlorophenoxyacetic acid by peroxymonosulfate/magnetic copper ferrite nanoparticles/ozone: a novel combination of advanced oxidation processes, Chem. Eng. J., 320 (2017) 436–447.

[8] M.A. Lemus, T. López, S. Recillas, D.M. Frías, M. Montes, J.J. Delgado, M.A. Centeno, J.A. Odriozola, Photocatalytic degradation of 2,4-dichlorophenoxyacetic acid using nanocrystalline cryptomelane composite catalysts, J. Mol. Catal. A: Chem., 281 (2008) 107–112.

[9] Y. Xi, M. Mallavarapu, R. Naidu, Adsorption of the herbicide 2,4-D on organo-palygorskite, Appl. Clay Sci., 49 (2010) 255–261.

[10] E.I. Seck, J.M. Doña-Rodríguez, C. Fernández-Rodríguez, O.M. González-Díaz, J. Araña, J. Pérez-Peña, Photocatalytic removal of 2,4-dichlorophenoxyacetic acid by using sol-gel synthesized nanocrystalline and commercial TiO_2: Operational parameters optimization and toxicity studies, Appl. Catal., B, 125 (2012) 28–34.

[11] WHO, Guidelines for Drinking-Water Quality, Vol. 1, Recommendations, 3rd ed., World Health Organization, Geneva, 2004.

[12] C.Y. Kwan, W. Chu, A study of the reaction mechanisms of the degradation of 2,4-dichlorophenoxyacetic acid by oxalate-mediated photooxidation, Water Res., 38 (2004) 4213–4221.

[13] S.C. Lee, N. Hasan, H.O. Lintang, M. Shamsuddin, L. Yuliati, Photocatalytic removal of 2,4-dichlorophenoxyacetic acid herbicide on copper oxide/titanium dioxide prepared by co-precipitation method, IOP Conf. Ser.: Mater. Sci. Eng., 107 (2016) 012012, doi: 10.1088/1757-899x/107/1/012012.

[14] A.M. Bello-Ramírez, B.Y. Carreón-Garabito, A.A. Nava-Ocampo, A theoretical approach to the mechanism of biological oxidation of organophosphorus pesticides, Toxicology, 149 (2000) 63–68.

[15] S.P. Kamble, S.P. Deosarkar, S.B. Sawant, J.A. Moulijn, V.G. Pangarkar, Photocatalytic degradation of 2,4-dichlorophenoxyacetic acid using concentrated solar radiation: batch and continuous operation, Ind. Eng. Chem. Res., 43 (2004) 8178–8187.

[16] E. Bazrafshan, F. Kord Mostafapour, H. Faridi, M. Farzadkia, S. Sargazi, A. Sohrabi, Removal of 2,4-dichlorophenoxyacetic acid (2,4-D) from aqueous environments using single-walled carbon nanotubes, Health Scope, 2 (2015) 39–46.

[17] M. Naushad, G. Sharma, Z.A. Alothman, Photodegradation of toxic dye using gum Arabic-crosslinked-poly(acrylamide)/$Ni(OH)_2$/FeOOH nanocomposites hydrogel, J. Cleaner Prod., 241 (2019) 118263, doi: 10.1016/j.jclepro.2019.118263.

[18] H. El Harmoudi, L. El Gaini, E. Daoudi, M. Rhazi, Y. Boughaleb, M.A. El Mhammedi, A. Migalska-Zalas, M. Bakasse, Removal of 2,4-D from aqueous solutions by adsorption processes using two biopolymers: chitin and chitosan and their optical properties, Opt. Mater., 36 (2014) 1471–1477.
[19] B.K. Jung, Z. Hasan, S.H. Jhung, Adsorptive removal of 2,4-dichlorophenoxyacetic acid (2,4-D) from water with a metal-organic framework, Chem. Eng. J., 234 (2013) 99–105.
[20] S.K. Deokar, S.A. Mandavgane, B.D. Kulkarni, Adsorptive removal of 2,4-dichlorophenoxyacetic acid from aqueous solution using bagasse fly ash as adsorbent in batch and packed-bed techniques, Clean Technol. Environ. Policy, 18 (2016) 1971–1983.
[21] A. Kumar, G. Sharma, A.H. Al-Muhtaseb, M. Naushad, A.A. Ghfar, C. Guo, F.J. Stadler, Biochar-templated g-C_3N_4/$Bi_2O_2CO_3$/$CoFe_2O_4$ nano-assembly for visible and solar assisted photo-degradation of paraquat, nitrophenol reduction and CO2 conversion, Chem. Eng. J., 339 (2018) 393–410.
[22] A. Kumar, G. Sharma, A.H. Al-Muhtaseb, M. Naushad, A.A. Ghfar, F.J. Stadler, Quaternary magnetic BiOCl/g-C_3N_4/Cu_2O/Fe_3O_4 nano-junction for visible light and solar powered degradation of sulfamethoxazole from aqueous environment, Chem. Eng. J., 334 (2018) 462–478.
[23] A. Kumar, Shalini, G. Sharma, M. Naushad, A. Kumar, S. Kalia, C. Guo, G.T. Mola, Facile hetero-assembly of superparamagnetic Fe_3O_4/$BiVO_4$ stacked on biochar for solar photo-degradation of methyl paraben and pesticide removal from soil, J. Photochem. Photobiol., A, 337 (2017) 118–131.
[24] T. Tatarchuk, N. Paliychuk, R.B. Bitra, A. Shyichuk, M.U. Naushad, I. Mironyuk, D. Ziółkowska, Adsorptive removal of toxic methylene blue and acid orange 7 dyes from aqueous medium using cobalt-zinc ferrite nanoadsorbents, Desal. Water Treat., 150 (2019) 374–385.
[25] S. Liu, M. Lim, R. Amal, TiO_2-coated natural zeolite: rapid humic acid adsorption and effective photocatalytic regeneration, Chem. Eng. Sci., 105 (2014) 46–52.
[26] T. Tatarchuk, A. Shyichuk, I. Mironyuk, M. Naushad, A review on removal of uranium(VI) ions using titanium dioxide based sorbents, J. Mol. Liq., 293 (2019) 111563, doi: 10.1016/j.molliq.2019.111563.
[27] B. Wang, G. Zhang, Z. Sun, S. Zheng, Synthesis of natural porous minerals supported TiO_2 nanoparticles and their photocatalytic performance towards Rhodamine B degradation, Powder Technol., 262 (2014) 1–8.
[28] N. Khalfaoui-Boutoumi, H. Boutoumi, H. Khalaf, B. David, Synthesis and characterization of TiO_2–montmorillonite/polythiophene-SDS nanocomposites: application in the sono-photocatalytic degradation of rhodamine 6G, Appl. Clay Sci., 80–81 (2013) 56–62.
[29] J. Castañeda-Contreras, V.F. Marañón-Ruiz, R. Chiu-Zárate, H. Pérez-Ladrón de Guevara, R. Rodriguez, C. Michel-Uribe, Photocatalytic activity of erbium-doped TiO_2 nanoparticles immobilized in macro-porous silica films, Mater. Res. Bull., 47 (2012) 290–295.
[30] K. Mamulová Kutláková, J. Tokarský, P. Kovář, S. Vojtěšková, A. Kovářová, B. Smetana, J. Kukutschová, P. Čapková, V. Matějka, Preparation and characterization of photoactive composite kaolinite/TiO_2, J. Hazard. Mater., 188 (2011) 212–220.
[31] H. Ichiura, T. Kitaoka, H. Tanaka, Removal of indoor pollutants under UV irradiation by a composite TiO_2–zeolite sheet prepared using a papermaking technique, Chemosphere, 50 (2003) 79–83.
[32] A. Taheri Najafabadi, F. Taghipour, Physicochemical impact of zeolites as the support for photocatalytic hydrogen production using solar-activated TiO_2-based nanoparticles, Energy Convers. Manage., 82 (2014) 106–113.
[33] E.P. Reddy, L. Davydov, P. Smirniotis, TiO_2-loaded zeolites and mesoporous materials in the sonophotocatalytic decomposition of aqueous organic pollutants: the role of the support, Appl. Catal., B, 42 (2003) 1–11.
[34] H. Zabihi-Mobarakeh, A. Nezamzadeh-Ejhieh, Application of supported TiO_2 onto Iranian clinoptilolite nanoparticles in the photodegradation of mixture of aniline and 2,4-dinitroaniline aqueous solution, J. Ind. Eng. Chem., 26 (2015) 315–321.
[35] F. Abdollah, S.M. Borghei, E. Moniri, S. Kimiagar, H.A. Panahi, Laser irradiation for controlling size of TiO_2-Zeolite nanocomposite in removal of 2,4-dichlorophenoxyacetic acid herbicide, Water Sci. Technol., 80 (2019) 864–873.
[36] A.H. Alwash, A.Z. Abdullah, N. Ismail, Elucidation of reaction behaviors in sonocatalytic decolorization of amaranth dye in water using zeolite Y co-incorporated with Fe and TiO_2, Adv. Chem. Eng. Sci., 03 (2013) 113–122.
[37] I. Mironyuk, T. Tatarchuk, M. Naushad, H. Vasylyeva, I. Mykytyn, Highly efficient adsorption of strontium ions by carbonated mesoporous TiO_2, J. Mol. Liq., 285 (2019) 742–753.
[38] J.I. Pérez-Martínez, J.M. Ginés, E. Morillo, M.L.G. Rodríguez, J.R. Moyano, 2,4-dichlorophenoxyacetic acid/partially methylated-β-cyclodextrin inclusion complexes, Environ. Technol., 21 (2000) 209–216.
[39] J.M. Ginés, J.I. Pérez-Martinez, M.J. Arias, J.R. Moyano, E. Morillo, A. Ruiz-Conde, P.J. Sánchez-Soto, Inclusion of the herbicide 2,4-dichlorophenoxyacetic acid (2,4-D) with β-cyclodextrin by different processing methods, Chemosphere, 33 (1996) 321–334.
[40] J.M. Salman, V.O. Njoku, B.H. Hameed, Batch and fixed-bed adsorption of 2,4-dichlorophenoxyacetic acid onto oil palm frond activated carbon, Chem. Eng. J., 174 (2011) 33–40.
[41] Y.F. Chao, P.C. Chen, S.L. Wang, Adsorption of 2,4-D on Mg/Al-NO_3 layered double hydroxides with varying layer charge density, Appl. Clay Sci., 40 (2008) 193–200.
[42] I. Mironyuk, T. Tatarchuk, H. Vasylyeva, M. Naushad, I. Mykytyn, Adsorption of Sr(II) cations onto phosphated mesoporous titanium dioxide: mechanism, isotherm and kinetics studies, J. Environ. Chem. Eng., 7 (2019) 103430, doi:10.1016/j.jece.2019.103430.
[43] Y. Liu, Some consideration on the Langmuir isotherm equation, Colloids Surf., A, 274 (2006) 34–36.
[44] D.H. Everett, Manual of symbols and terminology for physicochemical quantities and units, Appendix II: definitions, terminology and symbols in colloid and surface chemistry, Pure Appl. Chem., 31 (1972) 577–638.
[45] K.R. Hall, L.C. Eagleton, A. Acrivos, T. Vermeulen, Pore- and solid-diffusion kinetics in fixed-bed adsorption under constant-pattern conditions, Ind. Eng. Chem. Fundam., 5 (1966) 212–223.
[46] H. Freundlich, Über die adsorption in lösungen, Z. Phys. Chem., 57 (1907) 385–470.
[47] M.I. Temkin, V.M. Pyzhev, Kinetic of ammonia synthesis on promoted iron catalyst, Acta Phys. Chim., 12 (1940) 327–356.
[48] D.L.P.O. Redlich, A useful adsorption isotherm, J. Phys. Chem., 63 (1959) 1024–1026.
[49] S. Lagergreen, Zur theorie der sogenannten adsorption gelöster Stoffe, Z. Chem. Ind. Kolloide, 2 (1907) 15.
[50] Y.S. Ho, Adsorption of Heavy Metals from Waste Streams by Peat, Ph.D Thesis, University of Birmingham, Birmingham, UK, 1995.
[51] S. Nethaji, A. Sivasamy, G. Thennarasu, S. Saravanan, Adsorption of Malachite green dye onto activated carbon derived from *Borassus aethiopum* flower biomass, J. Hazard. Mater., 181 (2010) 271–280.
[52] K. Nejati, S. Davary, M. Saati, Study of 2,4-dichlorophenoxyacetic acid (2,4-D) removal by Cu-Fe-layered double hydroxide from aqueous solution, Appl. Surf. Sci., 280 (2013) 67–73.
[53] M. Dehghani, S. Nasseri, M. Karamimanesh, Removal of 2,4-dichlorophenolyxacetic acid (2,4-D) herbicide in the aqueous phase using modified granular activated carbon, J. Environ. Health Sci. Eng., 12 (2014) 28, doi: 10.1186/2052-336X-12-28.